Article

Not peer-reviewed version

Sustainable Synthesis and Photocatalytic Activity of Translucent ZnO Nanowires Using Moringa Seed Extract

Basílio José Augusto José * and Mahendra Devidas Shinde *

Posted Date: 25 July 2024

doi: 10.20944/preprints202407.2042.v1

Keywords: Translucent Zinc Oxide Nanowires; Moringa seeds; Photocatalytic activity

Article

Sustainable Synthesis and Photocatalytic Activity of Translucent ZnO Nanowires Using Moringa Seed Extract

Basílio José Augusto José [1] and Mahendra Devidas Shinde [2]

[1] Ph.D Scholar at School of Science, Sandip University, India & Assistant Professor at the Faculty of Science and Technology, Licungo University, Beira, Mozambique; bjose@unilicungo.ac.mz

[2] School of Engineering and Technology, Sandip University, Nashik, India; mahendra.shinde@sandipuniversity.edu.in

* Correspondence: bjose@unilicungo.ac.mz (B.J.A.J.); mahendra.shinde@sandipuniversity.edu.in (M.D.S.); Tel.: +258840658226(B.J.A.J.); +91 +9194206 00626 (M.D.S.)

Abstract: Background: The study demonstrates the sustainable synthesis of translucent zinc oxide (ZnO) nanowires using Moringa seed extract, highlighting eco-friendly and sustainable approaches. Methods: Characterization techniques such as X-ray diffraction (XRD), field emission scanning electron microscopy (FESEM), energy dispersive spectroscopy (EDS), transmission electron microscopy (TEM), and X-ray photoelectron spectroscopy (XPS) confirmed the formation of ZnO nanostructures with diverse morphologies, including nanowires and spherical clusters. Results: The synthesized ZnO nanowires exhibited remarkable photocatalytic activity, achieving over 89% degradation efficiency of methylene blue (MB) under UV light within 80 minutes, demonstrating their potential for wastewater treatment applications. Conclusions: The research findings support Sustainable Development Goals (SDGs) related to clean water, climate action, and life below water and on land, highlighting the role of eco-friendly nanostructures in environmental remediation. The dual advantage of Moringa seed extract, providing both a sustainable synthesis route and health benefits due to its rich content of vitamins and phytochemicals, underscores the potential of integrating natural resources in nanotechnology for environmental and health applications.

Keywords: Translucent Zinc Oxide Nanowires; Moringa seeds; Photocatalytic activity.

1. Introduction

Embarking on an exploration of the Horseradish tree, known by various names such as Moringa, Mulangay, Benzolive, and more, reveals a tree of profound significance belonging to the Moringaceae family. Spanning the continents of Africa, Arabia, South and East Asia, the Pacific and Caribbean islands, and South America, Moringa establishes its presence in diverse geographical landscapes [1]. Beyond its wide distribution, Moringa stands out for its renowned nutritional and medicinal attributes

Diving into the intricate world of phytochemicals, Moringa unfolds a tapestry rich in vital vitamins, including L-ascorbic acid (vitamin C), retinol (vitamin A), and niacin (vitamin B3). The composition extends to an impressive variety of flavonoids like quercetin, kaempferol, myricetin, and isorhamnetin, coupled with notable phenolic acids such as ellagic acid, gallic acid, chlorogenic acid, and caffeic acid. This intricate amalgamation, thoughtfully organized into five distinct groups (refer to Table 1), underscores not only the nutritional value but also the potential health benefits of Moringa. Moreover, these constituents play a significant role in the synthesis of ZnO NPs [2,3].

The surge in environmentally conscious materials has become a focal point for scientists in the realms of nanotechnology and materials science. This heightened interest holds particular significance in the current era, as the world confronts the profound implications of climate change and global warming. These issues have been extensively deliberated in various forums, including the

 doi:10.20944/preprints202407.2042.v1

recent COP27 held in Egypt, and align with Sustainable Development Goals (SDG 7, 11, and 13) [4–6].

Approaches dedicated to crafting such materials are often labelled as "green" when they involve the use of active components derived from natural sources, aiming to reduce toxicity levels. Alternatively, the term "eco-friendly" is applied when there is a concerted effort to balance product quality with the minimization of environmental impact during the synthesis process [7–12]. This emphasis on environmentally sustainable practices reflects a collective commitment to addressing global challenges through innovative and responsible material development.

Within the existing literature, a myriad of synthesis methods have been documented, encompassing both conventional approaches [13] and environmentally conscious methods such as green and eco-friendly synthesis [14–17] as illustrated in Figure 1.

Table 1. Moringa composition and role.

N0	Phytochemicals	Role	Mechanism of formation	Ref. No
1	Phytosterols	Stabilizers of Zinc Ions	Regulating particle size, morphology, and structure.	[18,19]
2	Flavonoids	Reduction of Zinc ions	Reduce zinc ions, transforming them into nanoparticles while mitigating undesired side reactions during synthesis.	[20,21]
3	Polyphenols	Reducing and stabilizers of Zn^{+2}	Coat the surface of nanoparticles to prevent clustering and facilitate the reduction of Zn^{+2}	[18,19,22]
4	Amino Acids and Proteins	Capping and stabilizer of Zn^{+2}	Incorporate into the ZnO surface to prevent the formation of clusters, simultaneously providing stabilization and reduction.	[18,20,21]
5	Lipids	Hydrophobicity of ZnO NPs	Mult-compatibility and wettability through interaction with the ZnO surface	[18,21,22]

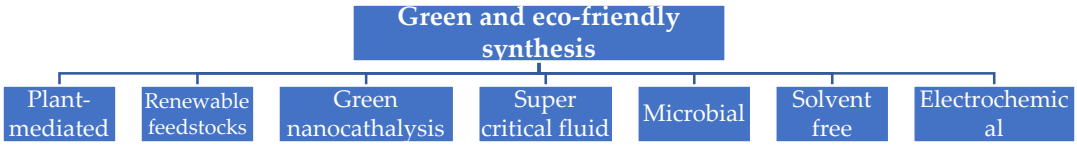

Figure 1. Green/Eco-friendly Synthesis of Nanoparticles .

1.1. Moringa Seeds Role in Synthesis of ZnO

The synthesis of zinc oxide (ZnO) utilizing Moringa seeds powder is orchestrated by a multitude of mechanisms, capitalizing on the synergistic and versatile roles played by phytochemicals. These intricate processes entail a dynamic interplay of biochemical compounds found in Moringa seeds, with each compound contributing to the synthesis in distinct yet interconnected ways. These roles encompass reduction, stabilization, capping, Ostwald ripening, and agglomeration, as illustrated in the Table 1.

Zinc Oxide (ZnO) stands out for its remarkable versatility, finding applications across diverse fields, including energy devices [23], biomedical applications [24–26], and sensing [27–29]. Ongoing research endeavors are dedicated to exploring environmentally friendly methods to harness the unique properties of ZnO. In the context of this experiment, we successfully synthesized high-quality ZnO nanostructures using [Zn $(CH_3COO)_2{\cdot}2H_2O$] and Moringa seed powder (MSP). A comprehensive characterization of these nanostructures covered their structural, surface, optical,

 doi:10.20944/preprints202407.2042.v1

electrochemical, and dielectric characteristics, with a specific focus on unraveling their potential applications in energy devices and nanofluids [3,30–32].

For the deposition of homogeneous thin films with high crystallinity on p-Si (100) using spin coating for photovoltaic materials, we employed green-synthesized ZnO nanoparticles from Punica granatum (pomegranate) juice extract [33]. Given that Punica belongs to the polyphenols group, the reaction with Zinc ions led to the formation of complex molecules of Zn $(OH)_2$ through a capping and reducing process. These complex molecules were transformed into respective nanoparticles during the annealing process at around 500°C. The resulting films exhibited a wurtzite hexagonal arrangement with a crystallite size of 60nm, a direct bandgap of 3.41eV according to UV-VIS Spectra, and a distribution of two components, Zn and O, as confirmed by EDX analysis. While the study did not extend to I-V and dielectric measurements, these findings lay the groundwork for potential applications of the films in light-emitting diodes apparatus.

For the fabrication of uniform, high-crystallinity thin films on p-Si (100) through spin coating in photovoltaic applications, a green synthesis of ZnO nanoparticles was undertaken utilizing Punica granatum (pomegranate) juice extract [33]. Within this process, Punica, classified under the polyphenols group, engaged in a reaction with Zinc ions, yielding complex Zn (OH)2 molecules through a capping and reducing process. These molecules underwent transformation into nanoparticles during the annealing process at approximately 500°C. The resultant films exhibited a wurtzite hexagonal arrangement with a crystallite size of 60nm, a direct bandgap of 3.41eV according to UV-VIS Spectra, and a distribution of two components, Zn and O, as confirmed by EDX analysis. Although the study omitted I-V and dielectric measurements, these findings lay the groundwork for potential applications of the films in light-emitting diode apparatus.

In recent investigations, ZnO was synthesized from various components of Moringa oleifera, including leaves [31,34] root extract [3] and seeds[14,32]. These green synthesis approaches primarily focused on exploring antimicrobial and photocatalytic activities. Particularly noteworthy is the utilization of Moringa oleifera seeds as a green-mediated agent, employed to synthesize Ag-ZnO NPs with a flower-like morphology, demonstrating efficacy against human pathogenic bacteria in nanotechnological and material science contexts.

Beyond the established findings, the crystalline structures of wurtzite (hexagonal) and zincite, coupled with their direct band gap ranging from 3.0 to 3.7 eV in their pure form, exceptional transparency, and adaptability, position green-synthesized ZnO NPs for promising applications in energy devices and storage [23] (thin films), enhancement of cement concrete properties [35–41] (powder and nanofluid), water purification [42–45] (nanofluids and thin films), engine coolants [46], EOR [47,48] (nano fluids), and gas sensors.

In the realm of green synthesis, the plant extract plays diverse roles. Operating as a reducing agent, the active components within the green material, when in an aqueous solution, facilitate the conversion of metal ions into their respective nanoparticles. Serving as stabilizers, these components act as surfactants to control the p of nanoparticles, mitigating their agglomeration. When extracts serve as capping agents, nucleation through aggregation occurs, giving rise to small clusters where the design of shape and size is meticulously orchestrated. During this intricate process, Ostwald ripening may take place, where larger particles grow at the expense of smaller particles through the diffusion of atoms [49–55] (Figure 1).

This experiment places special emphasis on the plant-mediated synthesis of ZnO nanoparticles (NPs) due to its myriad advantages. Plant-mediated synthesis is heralded for its environmental friendliness, reducing the reliance on excessive chemical usage. Moreover, it proves to be cost-effective, demanding fewer chemicals and materials. The method also stands out for its low toxicity, involving the use of smaller quantities of potentially harmful substances. The reliability of the plant-mediated synthesis method further distinguishes it, offering the convenience of a single-pot process, making it both practical and efficient [30,51,63].

In the process of green synthesis, the phytochemicals present in moringa engage with zinc ions, culminating in the formation of zinc oxide (ZnO) nanoparticles. These synthesized ZnO nanoparticles exhibit different morphologies and size resulting is various applications as illustrated in the Table 2.

 doi:10.20944/preprints202407.2042.v1

Table 2. Literature survey on synthesis and functionalization of ZnO using Moringa.

No	Eco-friendly synthesis	Cryst. Size	Applications	Ref. No.
1	Moringa seeds/Zinc precursor/Silver	36.187nm-54.1nm	Antibacterial activity	[56]
2	Moringa/seeds/flowers/ leaves/Zinc precursor	10.8nm-13.9	Study physical properties	[57]
3	Moringa leaves/Zinc percursor	0.98nm-91.51nm	Study physical properties	[58]
4	Moringa leaves/Zinc percursor	25nm	Photocatalytic activity of Titon yellow dye	[22]
7	Moringa seeds/Chitosan/Zinc percursor		Photocatalytic activity	[59]
8	Moringa leaves/Zinc percursor	9nm-18nm	Photocatalysis of wastewater petroleum refinery	[60]
9	Moringa leaves/Zinc percursor	52nm	Photocatalytic and antibacterial activity	[61]
10	Moringa roots/Zinc percursor	15nm-40nm	Antibacterial activity	[62]

2. Materials and Methods

For the experiment was used Zinc Acetate Dehydrate from Merck Life Science Private Limited with the product code ME2M712009, denoted as Zn $(CH_3COO)_2{\cdot}2H_2O$, ensuring a purity of over 98% and a molecular weight of 219.49 g/mol, classified under the reference UN3077. Moringa seeds, procured from Greenhouse Farm Services, Indrakunda Road, Panchavati, Nashik – 422003, underwent the subsequent processing steps as outlined in the (Figure 2), adhering strictly to the relevant guidelines [64,65]. For the synthesis process 10.97g of [Zn $(CH_3COO)_2{\cdot}2H_2O$] were directly combined with a 100ml solution of moringa aliquots extract described in the Figure 2, and stirred the mixture at 60°C for 1 hour. Sequentially, 0.7g of NaOH were added and the solution subjected to probe sonication for 15 minutes. Afterwards, the solution was allowed to precipitate for 3 hours, and the supernatant was separated from precipitate by using a syringe. The remaining white solution were transferred to a new beaker for washing with CH_3CH_2OH. After washing, the precipitant was removed using a syringe, and centrifuged at 3500 RPM for 5 minutes to allow proper separation. The precipitate material was transferred to a crucible and dried in an oven at 80°C for 48 hours. After complete drying, the obtained powder was subjected to calcination at 500°C for 2 hours to remove impurities and form ZnO [66]. Due to particle aggregation, the formed ZnO was ground multiple times using a mortar and pestle to obtain a fine powder (NPs), which was then stored in a 20ml brown glass bottle for characterization and further treatment. [51].

 doi:10.20944/preprints202407.2042.v1

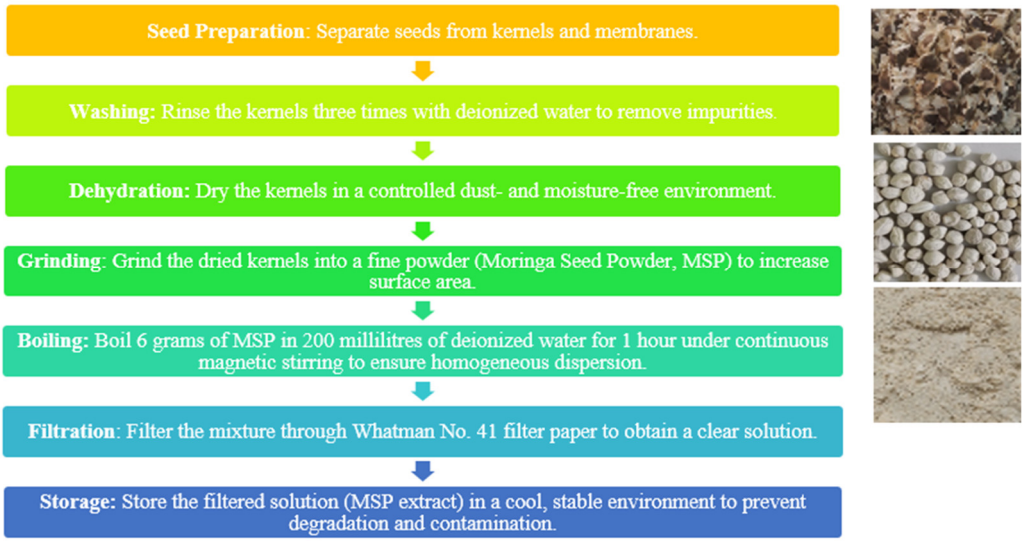

Figure 2. Moringa seeds preparation.

3. Results and Discussions

3.1. X-ray Diffraction Analysis

The structural characterization of ZnO was performed using X-ray diffraction (XRD) in the range of 20-80 degree (Figure 3). The obtained peaks were in accordance with the reference (JCPDS card N0. 75-1621) [67] indicating that the ZnO is related to hexagonal-wurtzite structure.

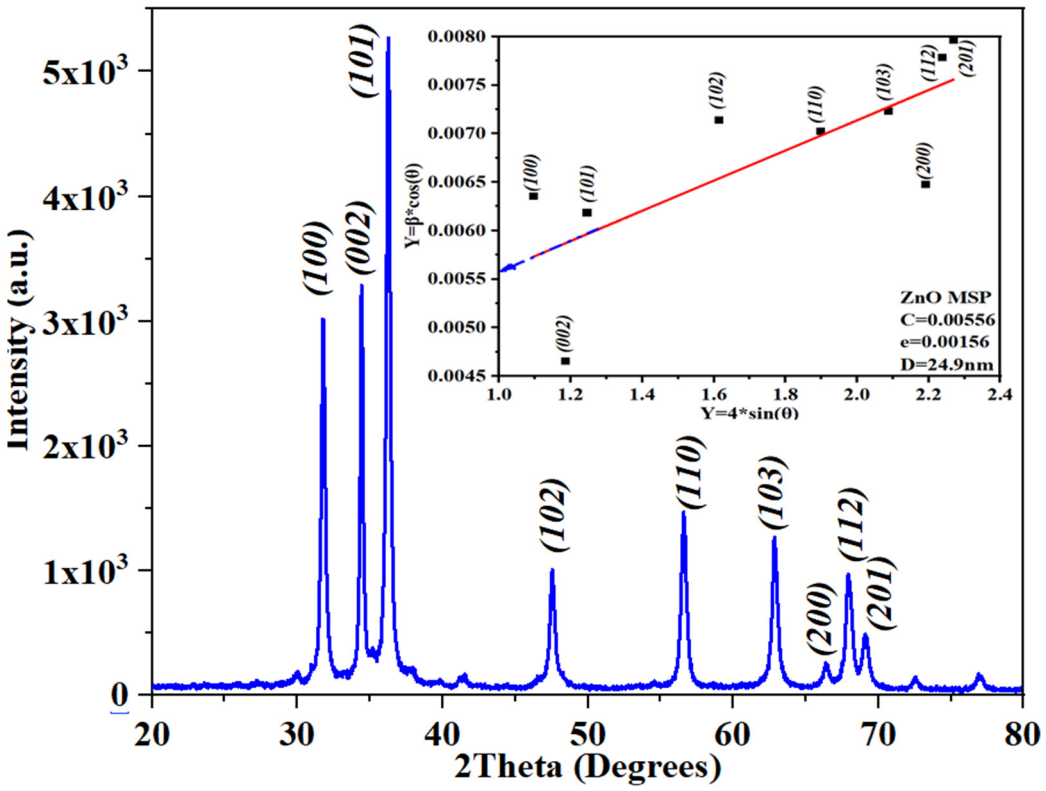

Figure 3. XRD diffraction patterns of ZnO.

As observed from the refined and fitted scattering pattern of the peaks, the average crystallite size was determined to be 20.9 nm using the Debye-Scherer formula. However, when applying the Williamson-Hall Plot, the average crystallite size was calculated as 24.9 nm.

 doi:10.20944/preprints202407.2042.v1

The discrepancy in the average crystallite size, by applying the two methods, arises from the distinct methodologies employed in these X-ray diffraction analysis techniques. The Debye-Scherer formula calculates size based primarily on peak broadening, assuming uniform strain distribution and minimal lattice imperfections. In contrast, the Williamson-Hall plot incorporates both crystallite size and strain effects on peak broadening, fitting parameters against scattering angle to account for variations in lattice strain. Consequently, the larger size estimate from the Williamson-Hall plot (24.9 nm) reflects its consideration of strain-related broadening in addition to crystallite size effects, highlighting the method's sensitivity to crystallographic imperfections and strain distribution within the sample [68].

3.2. Field Emission Scanning Electron Microscopy coupled with Energy Dispersive X-ray Spectroscopy image analysis.

To comprehensively confirm the TEM measurements, a surface morphology study was conducted on the sample synthesized using Moringa seeds. This analysis employed FESEM-EDX TESCAN with an electron beam landing energy ranging from 200 eV to 30 kV, a probe current from 2 pA to 400 nA, and magnification levels from 50x to 200,000x, utilizing the Octane Elite Super EDS detector.

Figures 4 and 5 illustrate various morphologies observed at both nanoscale and microscale levels. The images reveal the presence of sheet-like, rod-like, and spherical particles, often forming cluster-type structures. These diverse morphologies highlight the intricate and varied nature of the synthesized ZnO nanostructures, corroborating the findings from the TEM analysis and providing a more detailed understanding of their structural characteristics.

Figure 4. FESEM Nanowires at 500 nm resolution.

 doi:10.20944/preprints202407.2042.v1

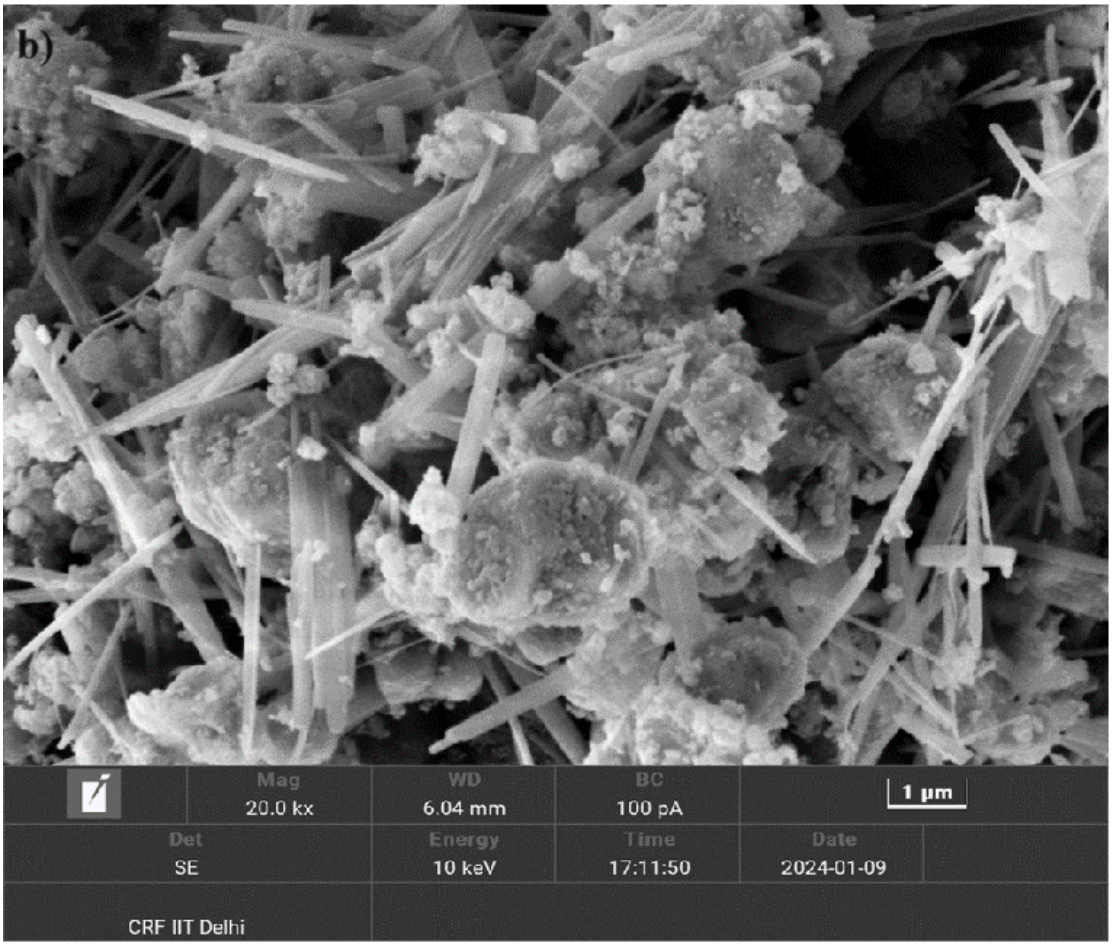

Figure 5. FESEM Sphere like growing alongside nanowires at 1µm resolution.

The eco-friendly synthesis method using Moringa seeds played a crucial role in the observed morphologies of the ZnO nanostructures. The natural phytochemicals present in Moringa seeds, such as proteins, alkaloids, and flavonoids, likely act as stabilizing and capping agents during the synthesis process, influencing the formation and growth of ZnO nanostructures [14,58]. The diverse morphologies observed—sheets, rods, and spherical particles, can be correlated to the specific interactions between the ZnO precursors and these moringa components. Sheet-like structures may form due to the planar adsorption of certain molecules on ZnO surfaces, promoting two-dimensional growth. Rod-like structures suggest anisotropic growth, which can occur when biomolecules selectively bind to specific crystal facets, directing growth along one axis. The formation of spherical particles indicates isotropic growth, where the biomolecules uniformly surround the ZnO nuclei, leading to a more balanced growth in all directions. The presence of these varied morphologies as clusters can be attributed to the aggregation properties of the nanostructures during the synthesis process. The clustering could result from the residual biomolecules acting as bridges between individual nanostructures, leading to the formation of larger assemblies.

The synthesis method using Moringa seeds significantly influenced the observed surface morphologies of ZnO nanostructures. The composition of moringa seeds facilitate the formation of distinct shapes and clusters, confirmed by the detailed surface morphology study, supporting the structural diversity indicated by the TEM measurements.

Based on Figure 6, the synthesis of ZnO nanostructures was successfully achieved through an eco-friendly process, as evidenced by the quasi-stoichiometric presence of zinc and oxygen with atomic percentages of 43.31% and 45.60%, respectively, as depicted in the spectrum obtained from EDS attached with FESEM. This near-stoichiometric ratio indicates a well-controlled synthesis method, crucial for maintaining the desired material properties.

 doi:10.20944/preprints202407.2042.v1

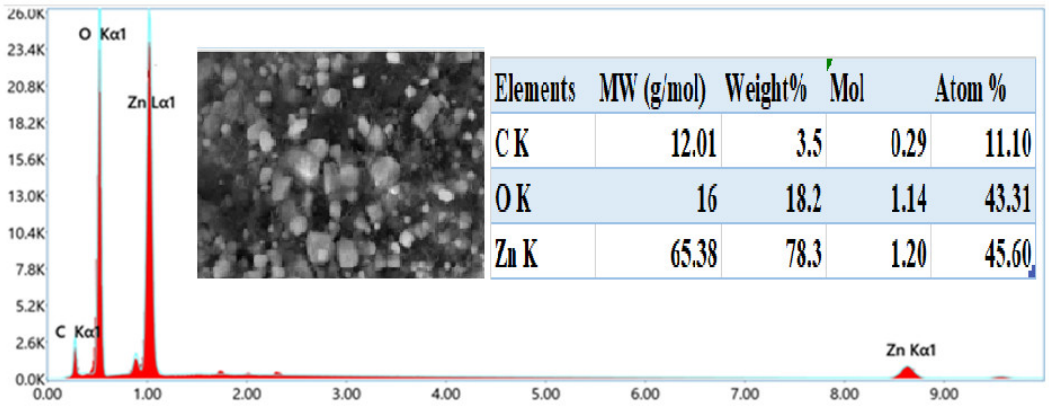

Elements	MW (g/mol)	Weight%	Mol	Atom %
C K	12.01	3.5	0.29	11.10
O K	16	18.2	1.14	43.31
Zn K	65.38	78.3	1.20	45.60

Figure 6. Elemental analysis using EDX of ZnO nanostructures.

The presence of carbon in the spectrum can be attributed to several factors. Firstly, it may originate from the carbon tape used during sample preparation and measurement, which can contribute to background signals. Additionally, carbon signals observed could result from adsorption from the surrounding environment during sample exposure. Another significant source of carbon is the organic matter present in Moringa seeds, such as phytosterols, flavonoids, polyphenols, amino acids, proteins, and lipids, all of which inherently contain carbon. These organic compounds likely play a role as stabilizing agents during the synthesis process, influencing the surface composition of the ZnO nanostructures.

The atomic percentages of zinc, oxygen, and carbon observed in the EDS spectrum are crucial for understanding the stoichiometry and composition of the synthesized ZnO nanostructures. The quasi-stoichiometric ratio of zinc and oxygen suggests that the synthesis method effectively controlled the elemental composition, which is vital for ensuring the desired properties of ZnO in various applications [81].

For instance, in photocatalysis, the stoichiometric balance between zinc and oxygen is crucial for enhancing the efficiency of light-induced reactions. Moreover, the presence of carbon revealed the potential surface modifications or functionalization that can be achieved through tailored synthesis methods involving organic precursors like Moringa seeds. These findings not only support the eco-friendly synthesis approach but also contribute to the broader understanding of nanomaterial synthesis and its applications in sustainable technology [82,83].

3.3. Transmission Electron Microscopy Analysis

Transmission Electron Microscopy (TEM) was conducted on sample. In Figure 7,8 and 9 various morphologies within the crystallites are illustrated, with nanowires predominantly present (Figure 8). Additionally, spherical-like in the form of clusters were identified in the micro and nano scale level, growing alongside the rods in a flower-like pattern (Figure 7).

 doi:10.20944/preprints202407.2042.v1

Figure 7. Flower-like Growth Along Wires ZnO Nanopaticles from TEM.

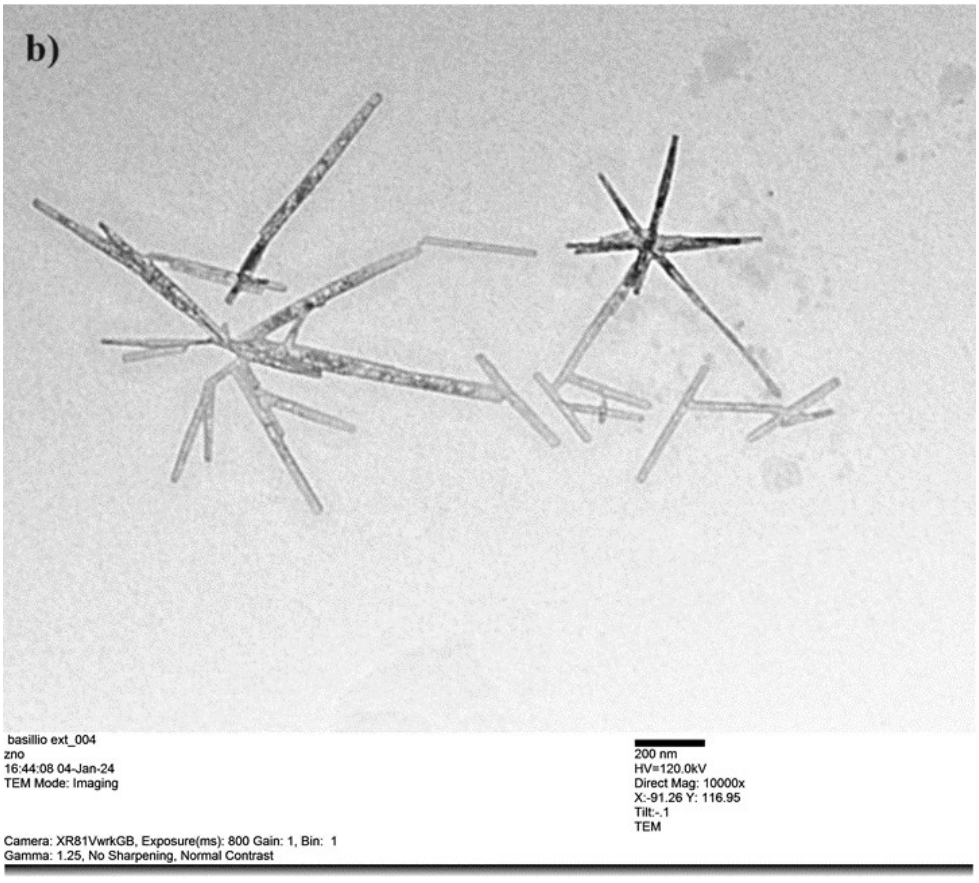

 doi:10.20944/preprints202407.2042.v1

Figure 8. Nanowires ZnO Nanopaticles from TEM.

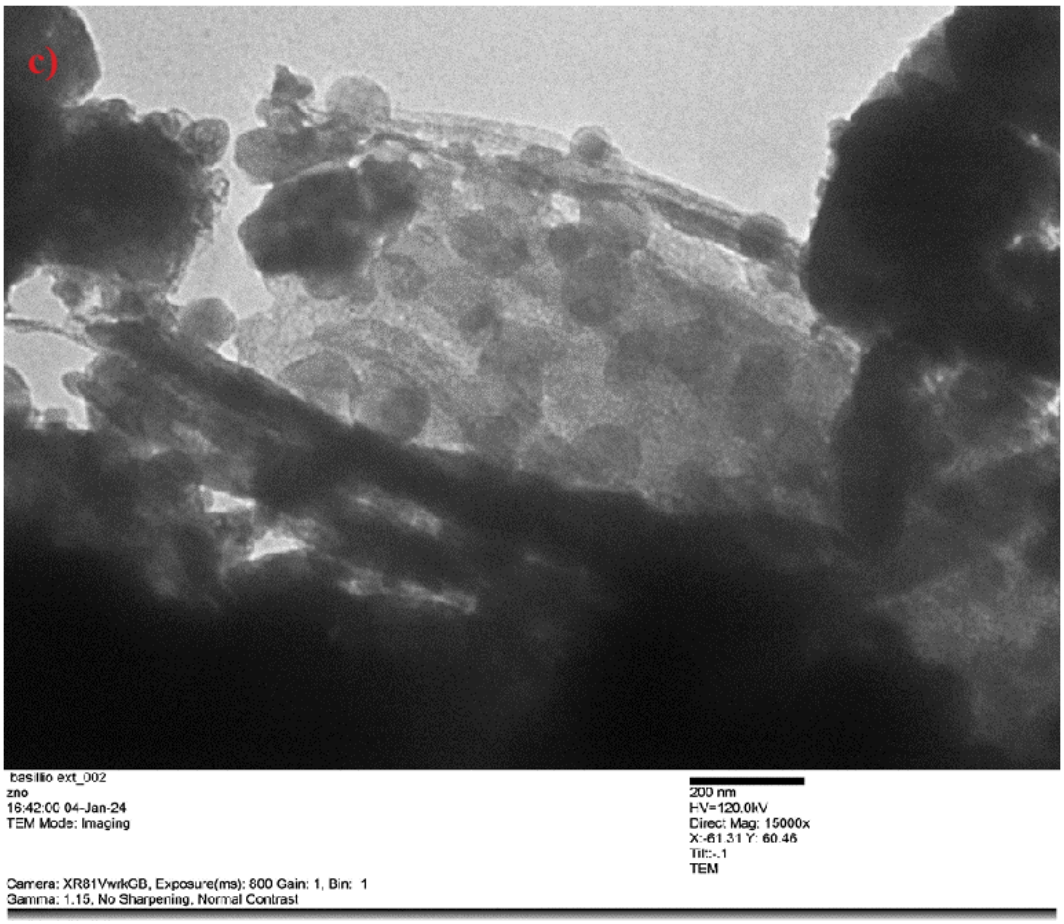

Figure 9. Spherical shape ZnO Nanopaticles from TEM.

The observed morphologies might be attributed to the pH (7,3) level of the reaction at room temperature (30°C) which defined the final structure of nanoparticles. Also, the organic compounds present in the moringa, including proteins, carbohydrates, and polyphenols described their role in the Table 1, might have acted as capping, stabilizers and reducing agents. These agents influence the growth direction and shape of ZnO nanostructures, leading to the formation of diverse morphologies [30].

The formation of translucent one-dimensional nanowires is favoured by anisotropic growth kinetics, driven by selective adsorption of stabilizing agents on specific crystallographic directions. In contrast, translucent spherical-like clusters and flower-like patterns likely might have aroused from secondary nucleation and hierarchical assembly of smaller nanoparticles (Ostwald ripening), influenced by the organic compounds in Moringa seed extract. By using DW as a solvent provided a controlled environment for ZnO crystallization, where factors like temperature and stirring might have shape the final morphology [57]. This interplay of precursor, moringa seed-derived and synthesis conditions at room temperature might have contributed to the varied structures observed in TEM images, displaying the advantages of sustainable synthesis approaches.

In the analyzed section of Figure 9, a detailed examination of crystallite sizes was conducted on 52,200 entities within the provided TEM image using the Feret's diameter concept in the ImageJ software particle analyzer. Feret's diameter, named after mathematician Joseph Feret, represents the longest dimension within an object along a specified direction, determined as the distance between two parallel lines tangent to the particle being measured [69–71].

In the analyzed section of Figure 9, a detailed examination of crystallite sizes was conducted on 52,200 entities within the provided TEM image using the Feret's diameter concept in the ImageJ

 doi:10.20944/preprints202407.2042.v1

software particle analyzer. Feret's diameter, named after mathematician Joseph Feret, represents the longest dimension within an object along a specified direction, determined as the distance between two parallel lines tangent to the particle being measured [69–71].

As illustrated in Figure 10, approximately 52,121 crystallites measured less than 20 nm, while only four crystallites ranged from 100 nm to 330 nm. This distribution confirms that the synthesized material falls within the nanostructure range, specifically classified as ZnO nanostructures.

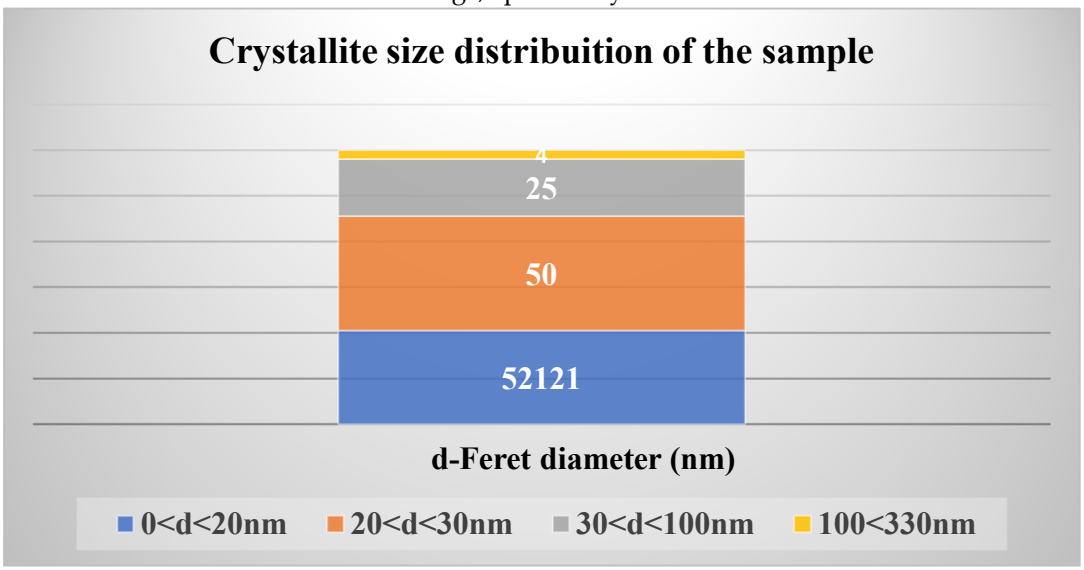

Figure 10. Crystallite size distribution of the sample.

3.4. X-ray Photoelectron Spectroscopy

The elemental composition, chemical state analysis, and surface characterization of the ZnO nanostructures were investigated using X-ray photoelectron spectroscopy (XPS), Figure 11. This analysis employed Al K-alpha (1486.61 eV) X-rays produced by a SPECS Surface Nano Analysis GmbH instrument, covering an energy range of 0-1300 eV. The XPS measurements were conducted with an acceleration voltage of 13 kV and a power of 100 W. XPS analysis yielded crucial insights into the elemental composition, oxidation states, and chemical bonding of the surface species present in the ZnO nanostructures [72].

 doi:10.20944/preprints202407.2042.v1

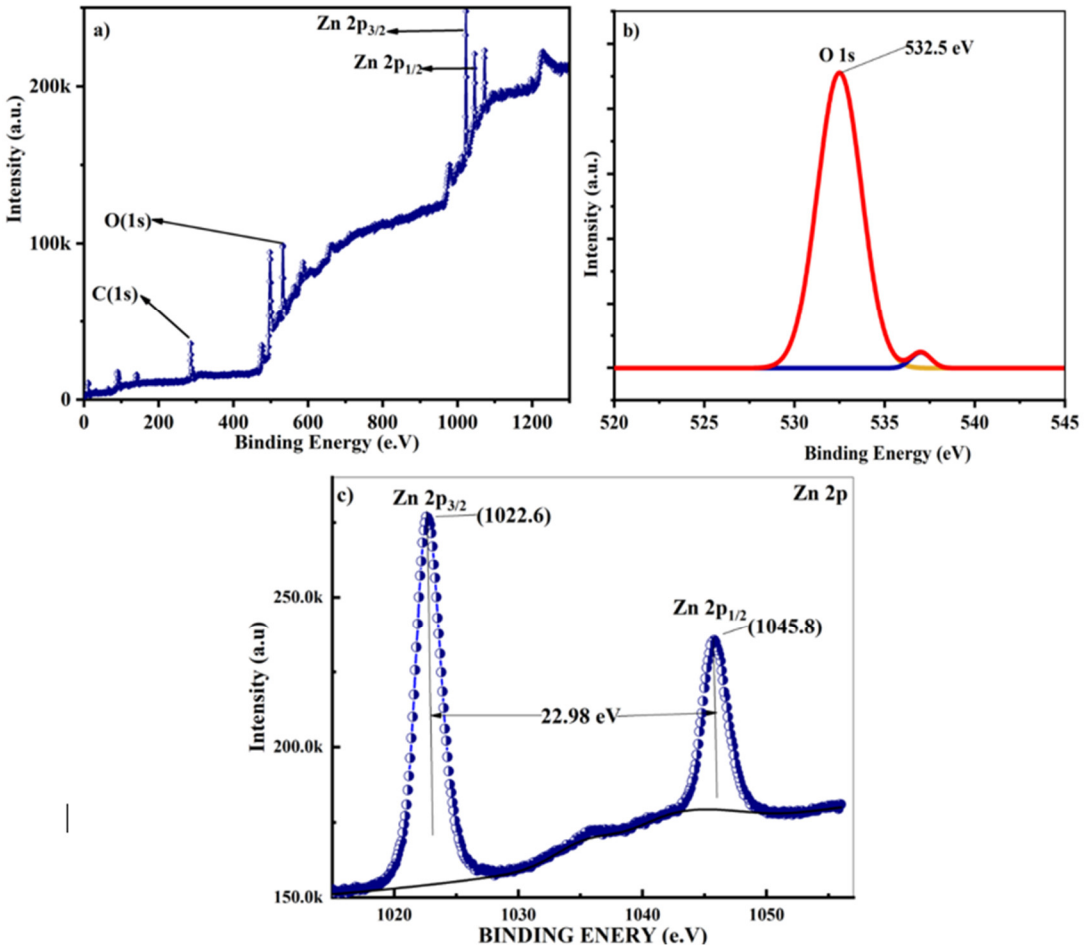

Figure 11. XPS patterns of ZnONPs (a) Full scan, (b) Oxygen 1s, (c) Zn 2p.

A comparison between the experimental data for Zinc and the theoretical data provided by [73], which reported the binding energy of L and M core levels for metals ranging from ^{22}Ti to ^{30}Zn, revealed slight differences of less than 0.1%. These minor discrepancies could be attributed to variations in the measuring instruments, as the reference data were obtained using a Hewlett-Packard 5950 A ESCA. Another potential reason could be the different methodologies employed; the reference data used chemical synthesis techniques from 1981, predating the advent of green synthesis approaches. Thus, while the data align closely, these minor differences highlight the impact of instrument and methodological variations on experimental results.

The XPS analysis, Figure 11, revealed two prominent peaks at 1022.5 eV and 1045.5 eV, corresponding to the Zn $2p_{3/2}$ (1022.0 eV) and Zn $2p_{1/2}$ (1045.1 eV) respectively, indicating Zn-O bonding within the hexagonal wurtzite structure [74,75]. These observations align with the core-electron binding energies reported for the first thirty elements. Additionally, Zn signals were detected at 9.8 eV (Zn 3d3/2, reference value: 9.77 eV), 91.5 eV (Zn $3p_{1/2}$, reference value: 91.4 eV), 142.5 eV (Zn 3s, reference value: 142.0 eV), and 1206.0 eV (Zn 2s).

Furthermore, in the spectrum, several other elements were identified, including 285.3 eV as (C 1s 285.0±0, 3), [76] for pure native elements, 535.2 eV as (O1s 532 eV), and 956.7 eV that might be related (Al 2s). Additionally, the peak at 1071.1 eV might be related to Na(1s) (1071,7±0,7) [72,77–80].

These results collectively confirm the presence and chemical states of Zn, C, and O within the nanostructures, thereby validating the structural integrity and chemical composition of the synthesized ZnO nanostructures.

3.5. Investigating Photocatalytic Activity of ZnO nanostructures

 doi:10.20944/preprints202407.2042.v1

The synthesized ZnO represents a significant advancement in promoting sustainable practices through eco-friendly synthesis and technological applications. Amid rising concerns over pollution and its detrimental effects on air and water quality, this research highlights the crucial role of eco-friendly synthesized ZnO nanostructures in mitigating environmental impacts. The study specifically investigates the photodegradation of methylene blue, a prevalent and harmful dye commonly discharged into wastewater by industries including textiles, printing, medicine, and laboratories.

The disposal of MB into wastewater, prior to proper pretreatment, poses threats to aquatic life, leads to water contamination, and disrupts ecosystems. Furthermore, direct exposure to humans can result in respiratory diseases, throat, eye, and skin irritation, as well as allergic reactions. In cases of ingestion, methylene blue may induce nausea, abdominal pains, and vomiting. The cumulative adverse effects necessitate the implementation of compensatory pretreatment measures for wastewater containing this dye.

Diverse formulations have been investigated for the degradation of methylene blue Table 4, but certain options are accompanied by undesirable side effects [92]. In light of its GRASE (generally recognized as safe and effective) status [93], research suggests that ZnO makes noteworthy contributions to the degradation of various dyes. This positions ZnO as a promising path for the development of environmentally friendly and sustainable wastewater treatment practices.

Table 4. Summary of ZnO Efficiency in Methylene Blue Removal: Previous Findings.

N0	ZnO Morphology	Cryst. Size	Effectiveness in MB removal	Ref
1	ZnO-NR	42.25nm	50% in 120min and 86% removal	[84]
2	ZnO ACF[1]/NR	42.25nm	99% removal after 120 minutes	[84]
3	ZnO/CNCs[2]	7.7-59.5nm	82.2% removal after 120 minutes	[85]
4	ZnO	7.7-59.5nm	65.87% removal after 120 minutes	[85]
5	Ag-ZnO	40-77nm	98% removal in 14-50 minutes	[86]
6	Green Synth./Citrus ZnO	10-35nm	120minutes removal	[87]
7	Green Synth./Myrtus ZnONW	10µm	99%removal	[88]
8	Green Synth./Tymus ZnO NPs	20-30nm	95% removal of real textile wastewater in 60 minutes under UV	[89]
9	Green Stynth. Plygonum minus ZnO/TiO_2	32nm/28nm	99.5% removal to ZnO and 90% to TiO_2 after 60 minutes	[90]
10	Green Stynth. Gomphrena serrata ZnO Spherical	20-30nm	90.5% removal after 180 minutes	[91]

1-ACF (Activated carbon fibers), 2-Cellulose nanocrystals.

3.5.1. Experimental Procedure and Results

Based on the research findings presented in Tables 2 and 4, laboratory experiments were conducted using eco-friendly methods to synthesize ZnO. This experiment employed light with a wavelength of λ = 395 nm to investigate the effectiveness of ZnO in degrading methylene blue (MB), as shown in Figure 12a. Centrifugation was used to remove residues from aliquots at each phase of the experiment (Figure 12b). Additionally, Figures 12c and 12d depict the initial and final states of the simulated wastewater.

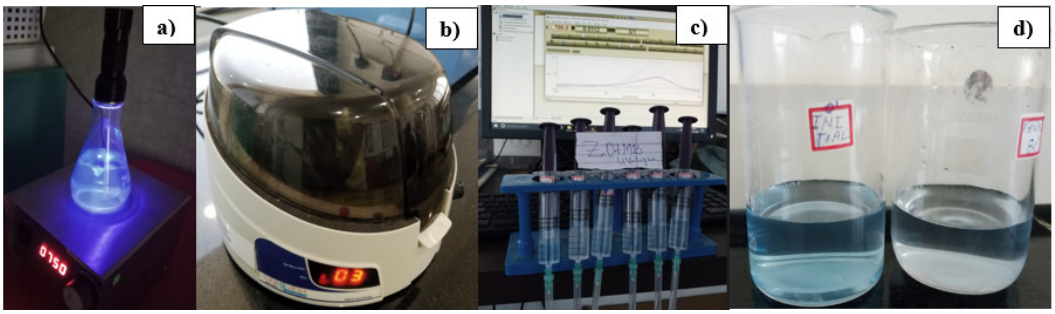

Figure 12. Experimental procedure of photodegradation testing.

 doi:10.20944/preprints202407.2042.v1

To perform the experiment, 25 mg of ZnO was dispersed in 100 ml of distilled water, and a separate solution was prepared by dissolving 0.5 ml of MB in an equal volume of distilled water. Subsequent measurements revealed significant. The initial absorbance readings of ZnO (AbsZnO) and AbsMB solutions were recorded within the 400nm-700nm range, yielding values of 0.0247838 for AbsZnO, displaying a linear profile, and 0.0926765% for AbsMB, exhibiting a Gaussian curve-like trend, as depicted in Figure 13.

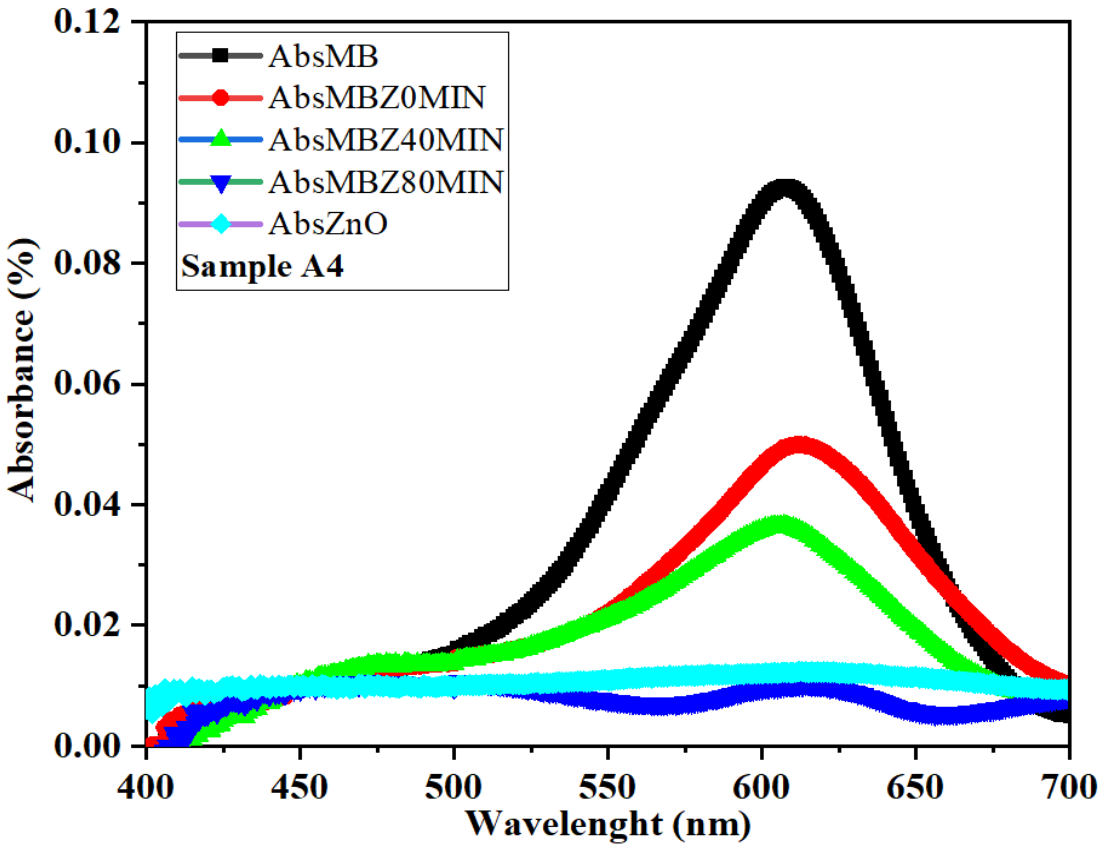

Figure 13. Absorbance Spectra of MB and (ZnO) Sample (A4) at 450-700nm.

Following the preparation, the ZnO solution was introduced into the Methylene Blue (MB) solution with vigorous magnetic stirring within a light-free environment. After a few minutes of blending, a 6ml aliquot was extracted using a syringe from the mixture, which has a cuvette capacity of approximately 3ml. This aliquot underwent centrifugation at 5000rpm for 3 minutes to settle any potential solid suspensions (Figure 12c). The resulting solution, denoted as AbsMBZ0, was measured for absorbance. Subsequently, the solution was exposed to UV light at 395nm (depicted in Figure 12a) with continuous vigorous magnetic stirring.

After a 40-minute UV exposure, another 6ml sample was collected, underwent centrifugation, and its absorbance was measured. A subsequent sample was collected after 80 minutes, at which point more than 89% of the initial Methylene Blue (MB) had already undergone degradation, as observed in Figure 14).

 doi:10.20944/preprints202407.2042.v1

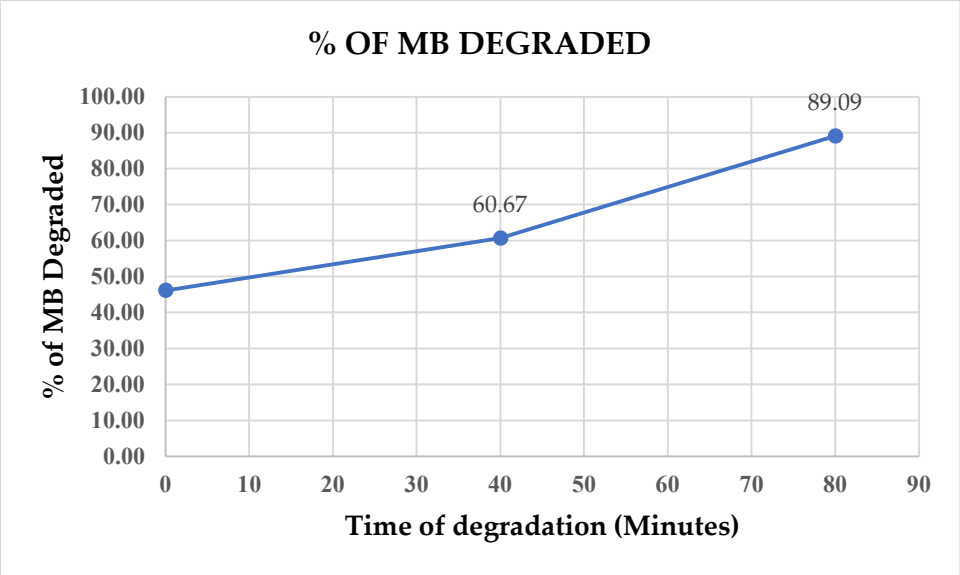

Figure 14. Dye Degradation Over Time: Temporal Evolution.

These findings highlight the promising potential of eco-friendly synthesized zinc oxide nanostructures in the pretreatment of wastewater containing methylene blue. This contribution is significant for addressing the challenges related to water pollution in both effluents and the broader environment. It aligns with key objectives outlined in Sustainable Development Goals, specifically SDG 6 (Clean Water and Sanitation), SDG 13 (Climate Action), SDG 14 (Life below Water), and SDG 15 (Life on Land) [94–96]

Conclusions

The study demonstrated the successful eco-friendly synthesis of zinc oxide (ZnO) nanostructures using Moringa seed extract, aligning with sustainable practices and contributing to green chemistry by reducing the environmental impact associated with conventional methods. The synthesized ZnO nanostructures exhibited significant photocatalytic activity, achieving over 89% degradation efficiency of methylene blue under UV light within 80 minutes, highlighting their potential for wastewater treatment applications. This research supports several Sustainable Development Goals (SDGs), notably SDG 6 (Clean Water and Sanitation), SDG 13 (Climate Action), SDG 14 (Life Below Water), and SDG 15 (Life on Land), by contributing to the reduction of water pollution and addressing environmental challenges. Characterization techniques such as TEM, XRD, and XPS confirmed the formation of ZnO nanostructures with diverse morphologies, including nanowires and spherical clusters, which are suitable for applications in optoelectronics, sensors, photovoltaic cells, and catalysis. The findings encourage further exploration into the environmental remediation applications of ZnO nanostructures and the continued development of sustainable synthesis methods using natural extracts, which could be applied to other metal oxides and nanomaterials. Additionally, the use of Moringa seed extract not only offers a sustainable synthesis route but also leverages the health benefits of Moringa, rich in vitamins and phytochemicals, underscoring the value of integrating natural resources into nanotechnology for both environmental and health applications.

Supplementary Materials: The following supporting information can be downloaded at the website of this paper posted on Preprints.org.

Author Contributions: The research was jointly conceptualized by B.J.A. José and M.D. Shinde. B.J.A. José prepared the methodology, handled characterization, and conducted formal analysis and investigation. Both authors contributed to data curation, resource collection, and visualization. B.J.A. José wrote the original draft, while M.D. Shinde reviewed the manuscript. Supervision and project

administration were managed by M.D. Shinde. B.J.A. José secured funding for characterization and resources acquisition. All authors have read and approved the final manuscript.

Funding: This research received no external funding.

Data Availability Statement: Data is available at UGC-DAE-CSR Indore https://www.csruserportal.com/Intro/userListIndore, (XRD and XPS characterization) and CRF IIT Delhi, https://crf.iitd.ac.in/, (TEM, FESEM, and EDS analyses). Also may be quickly observed from the link: https://drive.google.com/drive/folders/1lL4uJPIe_2nj9L4U_Fuqz4sQwrLzdmW8?usp=sharing

Acknowledgments: We gratefully acknowledge Sandip University for providing laboratory facilities, and UGC-DAE-CSR Indore for access to XRD and XPS characterization. We also extend our thanks to Licungo University, Mozambique, for their support. Additionally, we appreciate the CRF IIT Delhi for providing access to instruments such as TEM, FESEM, and EDS.

Conflicts of Interest: The authors declare no conflicts of interest.

References

1. Faizal A, Razis A. Health Benefits of Moringa oleifera. Moringa Oleifera Asian Pac J Cancer Prev n.d.;15:8571–6. https://doi.org/10.7314/APJCP.2014.15.20.8571.
2. Gopalakrishnan L, Doriya K, Kumar DS. Moringa oleifera: A review on nutritive importance and its medicinal application. Food Science and Human Wellness 2016;5:49–56. https://doi.org/10.1016/J.FSHW.2016.04.001.
3. Espenti CS, Rama Krishna AG, Rami Reddy Y V. Green biosynthesis of ZnO nanomaterials and their anti-bacterial activity by using Moringa Oleifera root aqueous extract. SN Appl Sci 2020;2:1–11. https://doi.org/10.1007/S42452-020-2945-3/TABLES/2.
4. Secretary-General's remarks to High-Level opening of COP27 | United Nations Secretary-General n.d. https://www.un.org/sg/en/content/sg/speeches/2022-11-07/secretary-generals-remarks-high-level-opening-of-cop27 (accessed November 20, 2022).
5. Atwoli L, Erhabor GE, Gbakima AA, Haileamlak A, Ntumba JMK, Kigera J, et al. COP27 Climate Change Conference: urgent action needed for Africa and the world. Lancet Oncol 2022;23:1486–8. https://doi.org/10.1016/S1470-2045(22)00645-3.
6. Zielinski C. COP27 Climate Change Conference: Urgent action needed for Africa and the world. Https://DoiOrg/101177/02692163221134453 2022;37:7–9. https://doi.org/10.1177/02692163221134453.
7. ECO-FRIENDLY | English meaning - Cambridge Dictionary n.d. https://dictionary.cambridge.org/dictionary/english/eco-friendly (accessed May 21, 2023).
8. Mohamed AA, Abu-Elghait M, Ahmed NE, Salem SS. Eco-friendly Mycogenic Synthesis of ZnO and CuO Nanoparticles for In Vitro Antibacterial, Antibiofilm, and Antifungal Applications. Biol Trace Elem Res 2021;199. https://doi.org/10.1007/s12011-020-02369-4.
9. Elemike EE, Onwudiwe DC, Singh M. Eco-friendly Synthesis of Copper Oxide, Zinc Oxide and Copper Oxide–Zinc Oxide Nanocomposites, and Their Anticancer Applications. J Inorg Organomet Polym Mater 2020;30. https://doi.org/10.1007/s10904-019-01198-w.
10. Almeida WL de, Rodembusch FS, Ferreira NS, Caldas de Sousa V. Eco-friendly and cost-effective synthesis of ZnO nanopowders by Tapioca-assisted sol-gel route. Ceram Int 2020;46. https://doi.org/10.1016/j.ceramint.2020.01.095.
11. Alahdal FAM, Qashqoosh MTA, Manea YK, Salem MAS, Khan AMT, Naqvi S. Eco-friendly synthesis of zinc oxide nanoparticles as nanosensor, nanocatalyst and antioxidant agent using leaf extract of P. austroarabica. OpenNano 2022;8. https://doi.org/10.1016/j.onano.2022.100067.
12. Li X, Natsuki J, Natsuki T. Eco-friendly synthesis of symmetrical pyramid structured zinc oxide nanoparticles and high temperature stable UV-shielding properties of zinc oxide /polyurethane composite membranes. Physica E Low Dimens Syst Nanostruct 2021;130:114677. https://doi.org/10.1016/J.PHYSE.2021.114677.
13. Abid N, Khan AM, Shujait S, Chaudhary K, Ikram M, Imran M, et al. Synthesis of nanomaterials using various top-down and bottom-up approaches, influencing factors, advantages, and disadvantages: A review. Adv Colloid Interface Sci 2022;300:102597. https://doi.org/10.1016/J.CIS.2021.102597.
14. José BJA, Shinde MD. Colloidal stability and dielectric behavior of eco-friendly synthesized zinc oxide nanostructures from Moringa seeds. Sci Rep 2024;14:2310. https://doi.org/10.1038/s41598-024-52093-5.
15. José BJA, Shinde MD, Bhavsar A. Eco-Friendly Synthesis of Zinc Oxide Nanostructures from Chicken Eggshell: Exploring Electrical and Colloidal Properties. INDIAN JOURNAL OF TECHNICAL EDUCATION 2024;47:34–8.

16. José BJA, Shinde MD, Azuranahim CAC. Zinc oxide nanostructures: review of eco-friendly synthesis and technological applications. Nanomaterials and Energy 2023;12:117–30. https://doi.org/10.1680/jnaen.23.00018.
17. Barzinjy AA, Hamadamen VN. Investigating Physical Properties and Formation Mechanism of Biosynthesized Zinc Oxide Nanoparticles using Dill (Anethum graveolens) Leaf Extract. Nanoscience & Nanotechnology-Asia 2022;12. https://doi.org/10.2174/2210681213666221114094914.
18. Stadtlander T, Becker K. Proximate Composition, Amino and Fatty Acid Profiles and Element Compositions of Four Different Moringa Species. Journal of Agricultural Science 2017;9:46. https://doi.org/10.5539/jas.v9n7p46.
19. Cattan Y, Patil D, Vaknin Y, Rytwo G, Lakemond C, Benjamin O. Characterization of Moringa oleifera leaf and seed protein extract functionality in emulsion model system. Innovative Food Science and Emerging Technologies 2022;75. https://doi.org/10.1016/j.ifset.2021.102903.
20. Bocarando-Guzmán MD, Luna-Suárez S, Hernández-Cázares AS, Herrera-Corredor JA, Hidalgo-Contreras JV, Ríos-Corripio MA. Comparison of the physicochemical and functional properties of flour and protein isolate from moringa (Moringa oleifera Lam.) leaves. Int J Food Prop 2022;25:733–47. https://doi.org/10.1080/10942912.2022.2058533.
21. Aderinola TA, Alashi AM, Nwachukwu ID, Fagbemi TN, Enujiugha VN, Aluko RE. In vitro digestibility, structural and functional properties of Moringa oleifera seed proteins. Food Hydrocoll 2020;101:105574. https://doi.org/10.1016/J.FOODHYD.2019.105574.
22. Letsholathebe D, Thema FT, Mphale K, Maabong K, Maria Magdalane C. Green synthesis of ZnO doped Moringa oleifera leaf extract using Titon yellow dye for photocatalytic applications. Mater Today Proc 2021;36:475–9. https://doi.org/10.1016/J.MATPR.2020.05.119.
23. Das HS, Mishra S, Dash MK, N PK, i, Maity SK, et al. Transparent Conducting Gallium-Doped Zinc Oxide Thin Films on Glass Substrate for Optoelectronic Device Applications. Https://WwwEspublisherCom/ 2023. https://doi.org/10.30919/ESMM5F841.
24. Jiang J, Pi J, Cai J, Fanizzi FP. The Advancing of Zinc Oxide Nanoparticles for Biomedical Applications 2018. https://doi.org/10.1155/2018/1062562.
25. Jiang J, Pi J, Cai J. The Advancing of Zinc Oxide Nanoparticles for Biomedical Applications. Bioinorg Chem Appl 2018;2018. https://doi.org/10.1155/2018/1062562.
26. Vijayakumar N, Bhuvaneshwari VK, Ayyadurai GK, Jayaprakash R, Gopinath K, Nicoletti M, et al. Green synthesis of zinc oxide nanoparticles using Anoectochilus elatus, and their biomedical applications. Saudi J Biol Sci 2022;29. https://doi.org/10.1016/j.sjbs.2021.11.065.
27. Patil LA, Bari AR, Shinde MD, Deo V. Ultrasonically prepared nanocrystalline ZnO thin films for highly sensitive LPG sensing. Sens Actuators B Chem 2010;149:79–86. https://doi.org/10.1016/J.SNB.2010.06.027.
28. Patil LA, Bari AR, Shinde MD, Deo V. Effect of pyrolysis temperature on structural, microstructural and optical properties of nanocrystalline ZnO powders synthesised by ultrasonic spray pyrolysis technique. J Exp Nanosci 2011;6. https://doi.org/10.1080/17458080.2010.509871.
29. Patil LA, Bari AR, Shinde MD, Deo V. Ultrasonically synthesized nanocrystalline ZnO powder-based thick film sensor for ammonia sensing. Sensor Review 2010;30. https://doi.org/10.1108/02602281011072161.
30. Matinise N, Fuku XG, Kaviyarasu K, Mayedwa N, Maaza M. ZnO nanoparticles via Moringa oleifera green synthesis: Physical properties & mechanism of formation. Appl Surf Sci 2017;406:339–47. https://doi.org/10.1016/J.APSUSC.2017.01.219.
31. Letsholathebe D, Thema FT, Mphale K, Maabong K, Maria Magdalane C. Green synthesis of ZnO doped Moringa oleifera leaf extract using Titon yellow dye for photocatalytic applications. Mater Today Proc 2021;36:475–9. https://doi.org/10.1016/J.MATPR.2020.05.119.
32. Swati, Verma R, Chauhan A, Shandilya M, Li X, Kumar R, et al. Antimicrobial potential of ag-doped ZnO nanostructure synthesized by the green method using moringa oleifera extract. J Environ Chem Eng 2020;8:103730. https://doi.org/10.1016/J.JECE.2020.103730.
33. Barzinjy AA, Hamad SM, Esmaeel MM, Aydin SK, Hussain FHS. Biosynthesis and characterisation of zinc oxide nanoparticles from Punica granatum (pomegranate) juice extract and its application in thin films preparation by spin-coating method. Micro Nano Lett 2020;15:415–20. https://doi.org/10.1049/MNL.2019.0501.
34. Elumalai K, Velmurugan S, Ravi S, Kathiravan V, Ashokkumar S. RETRACTED: Green synthesis of zinc oxide nanoparticles using Moringa oleifera leaf extract and evaluation of its antimicrobial activity. Spectrochim Acta A Mol Biomol Spectrosc 2015;143:158–64. https://doi.org/10.1016/J.SAA.2015.02.011.
35. Ghahari SA, Ghafari E, Hou P, Lu N. Hydration Properties of Cement Pastes with Al-Zinc Oxide and Zinc Oxide Nanoparticles. ES Materials and Manufacturing 2018;2:51–9. https://doi.org/10.30919/ESMM5F172.
36. Thangapandi K, Anuradha R, Awoyera PO, Gobinath R, Archana N, Berlin M, et al. Durability Phenomenon in Manufactured Sand Concrete: Effects of Zinc Oxide and Alcofine on Behaviour. Silicon 2021;13. https://doi.org/10.1007/s12633-020-00494-2.

37. Firasath Ali M, Talha Rashed M, Abdul Bari M, Mohammed Razi K. Effect of Zinc Oxide Nanoparticle on Properties of Concrete. International Research Journal of Engineering and Technology 2020.
38. Ali MF, Rashed MT, Bari MA, Razi KM. Effect of Zinc Oxide Nanoparticle on Properties of Concrete. International Reserach Journal of Engineering and Technology (IRJET) 2020;7.
39. Thangapandi K, Anuradha R, Archana N, Muthuraman P, Awoyera Paul O, Gobinath R. Experimental Study on Performance of Hardened Concrete Using Nano Materials. KSCE Journal of Civil Engineering 2020;24. https://doi.org/10.1007/s12205-020-0871-y.
40. Elia HN, Nima ZA. Self-cleaning concrete doped with nano and micro-size zinc oxide particles. vol. 15. 2019.
41. Dahesh AZ, Othman FM, Abdullah-Hamead AA. Improve mass concrete by controlling the crack sealing mechanism using microcapsules of zinc oxide. Materials Science Forum 2020;1002. https://doi.org/10.4028/www.scientific.net/MSF.1002.541.
42. Spoială A, Ilie C-I, Trușcă R-D, Oprea O-C, Surdu V-A, Vasile B Ștefan, et al. Zinc Oxide Nanoparticles for Water Purification. Materials 2021;14. https://doi.org/10.3390/ma14164747.
43. Gita S, Hussan A, Choudhury TG. Impact of Textile Dyes Waste on Aquatic Environments and its Treatment . Environment & Ecology 2017;3.
44. Weldegebrieal GK. Synthesis method, antibacterial and photocatalytic activity of ZnO nanoparticles for azo dyes in wastewater treatment: A review. Inorg Chem Commun 2020;120. https://doi.org/10.1016/j.inoche.2020.108140.
45. Fazil AA, Narayanan S, Begum MS, Manikandan G, Yuvashree M. Green synthesis strategy for producing doped and undoped ZnO nanoparticles: their photocatalytic studies for industrial dye degradation. Water Science and Technology 2021;84. https://doi.org/10.2166/wst.2021.308.
46. Ahmad H, Al-Khaled K, Sowayan AS, Abdullah M, Hussain M, Hammad A, et al. Experimental investigation for automotive radiator heat transfer performance with ZnO–Al2O3/water-based hybird nanoparticles: An improved thermal model. Https://DoiOrg/101142/S0217979223500509 2022;37. https://doi.org/10.1142/S0217979223500509.
47. Khazaei M, Hosseini MS, moshfegh Haghighi A, Misaghi M. IMPROVING THE PERFORMANCE OF ZNO NANOPARTICLES FOR EOR IN HIGH-TEMPERATURE AND HIGH SALINITY CARBONATE RESERVOIRS. J Porous Media 2023;26. https://doi.org/10.1615/JPORMEDIA.2023043520.
48. El-Masry JF, Bou-Hamdan KF, Abbas AH, Martyushev DA. A Comprehensive Review on Utilizing Nanomaterials in Enhanced Oil Recovery Applications. Energies 2023, Vol 16, Page 691 2023;16:691. https://doi.org/10.3390/EN16020691.
49. Hamad Azeez H, Barzinjy AA. Biosynthesis zinc oxide nanoparticles using Apium graveolens L. leaf extract and its use in removing the organic pollutants in water 2020. https://doi.org/10.5004/dwt.2020.25648.
50. Hamad Azeez H, Barzinjy AA. Biosynthesis zinc oxide nanoparticles using Apium graveolens L. leaf extract and its use in removing the organic pollutants in water 2020. https://doi.org/10.5004/dwt.2020.25648.
51. Barzinjy AA, Azeez HH. Green synthesis and characterization of zinc oxide nanoparticles using Eucalyptus globulus Labill. leaf extract and zinc nitrate hexahydrate salt. SN Appl Sci 2020;2:1–14. https://doi.org/10.1007/S42452-020-2813-1/FIGURES/14.
52. Azeez MA, Orege JI, Azeez MA, Orege JI. Bamboo, Its Chemical Modification and Products. Bamboo - Current and Future Prospects 2018. https://doi.org/10.5772/INTECHOPEN.76359.
53. Barzinjy AA, Azeez HH, Barzinjy AA, Hamad SM. Structure, Synthesis and Applications of ZnO Nanoparticles: A Review 2020;13:123–35. https://doi.org/10.47011/13.2.4.
54. Azeez AB, Samir MH, Haidar JI. Characterization of ZnO Nanoparticles Prepared from Green Synthesis Using Euphorbia Petiolata Leaves. Eurasian Journal of Science and Engineering 2019;4. https://doi.org/10.23918/eajse.v4i3sip74.
55. Barzinjy AA, Hamad SM, Abdulrahman AF, Biro SJ, Ghafor AA. Biosynthesis, Characterization and Mechanism of Formation of ZnO Nanoparticles Using Petroselinum Crispum Leaf Extract. Curr Org Synth 2020;17:558–66. https://doi.org/10.2174/1570179417666200628140547.
56. Swati, Verma R, Chauhan A, Shandilya M, Li X, Kumar R, et al. Antimicrobial potential of ag-doped ZnO nanostructure synthesized by the green method using moringa oleifera extract. J Environ Chem Eng 2020;8. https://doi.org/10.1016/j.jece.2020.103730.
57. Ngom I, Ngom BD, Sackey J, Khamlich S. Biosynthesis of zinc oxide nanoparticles using extracts of Moringa Oleifera: Structural & optical properties. Mater Today Proc, vol. 36, Elsevier Ltd.; 2019, p. 526–33. https://doi.org/10.1016/j.matpr.2020.05.323.
58. Abel S, Tesfaye JL, Nagaprasad N, Shanmugam R, Dwarampudi LP, Krishnaraj R. Synthesis and Characterization of Zinc Oxide Nanoparticles Using Moringa Leaf Extract. J Nanomater 2021;2021:4525770. https://doi.org/10.1155/2021/4525770.
59. Roy H, Islam MdS, Arifin MT, Firoz SH. Chitosan-ZnO decorated Moringa oleifera seed biochar for sequestration of methylene blue: Isotherms, kinetics, and response surface analysis. Environ Nanotechnol Monit Manag 2022;18:100752. https://doi.org/https://doi.org/10.1016/j.enmm.2022.100752.

60. El Golli A, Contreras S, Dridi C. Bio-synthesized ZnO nanoparticles and sunlight-driven photocatalysis for environmentally-friendly and sustainable route of synthetic petroleum refinery wastewater treatment. Sci Rep 2023;13. https://doi.org/10.1038/s41598-023-47554-2.
61. Pal S, Mondal S, Maity J, Mukherjee R. Synthesis and Characterization of ZnO Nanoparticles using Moringa Oleifera Leaf Extract: Investigation of Photocatalytic and Antibacterial Activity. vol. 14. 2018.
62. Espenti CS, Rama Krishna AG, Rami Reddy Y V. Green biosynthesis of ZnO nanomaterials and their anti-bacterial activity by using Moringa Oleifera root aqueous extract. SN Appl Sci 2020;2. https://doi.org/10.1007/s42452-020-2945-3.
63. Barzinjy AA, Hamadamen VN. Investigating Physical Properties and Formation Mechanism of Biosynthesized Zinc Oxide Nanoparticles using Dill (Anethum graveolens) Leaf Extract. Nanoscience & Nanotechnology-Asia 2022;12. https://doi.org/10.2174/2210681213666221114094914.
64. McNutt MK, Bradford M, Drazen JM, Hanson B, Howard B, Jamieson KH, et al. Transparency in authors' contributions and responsibilities to promote integrity in scientific publication. Proc Natl Acad Sci U S A 2018;115:2557–60. https://doi.org/10.1073/PNAS.1715374115.
65. Editorial and publishing policies | Scientific Reports n.d. https://www.nature.com/srep/journal-policies/editorial-policies#research-involving-plants (accessed August 22, 2023).
66. Fakhari S, Jamzad M, Kabiri Fard H. Green synthesis of zinc oxide nanoparticles: a comparison. Green Chem Lett Rev 2019;12. https://doi.org/10.1080/17518253.2018.1547925.
67. Iqbal T, Raza A, Zafar M, Afsheen S, Kebaili I, Alrobei H. Plant-mediated green synthesis of zinc oxide nanoparticles for novel application to enhance the shelf life of tomatoes. Applied Nanoscience (Switzerland) 2022;12. https://doi.org/10.1007/s13204-021-02238-z.
68. Mustapha S, Ndamitso MM, Abdulkareem AS, Tijani JO, Shuaib DT, Mohammed AK, et al. Comparative study of crystallite size using Williamson-Hall and Debye-Scherrer plots for ZnO nanoparticles. Advances in Natural Sciences: Nanoscience and Nanotechnology 2019;10:045013. https://doi.org/10.1088/2043-6254/AB52F7.
69. WALTON WH. Feret's Statistical Diameter as a Measure of Particle Size. Nature 1948;162:329–30. https://doi.org/10.1038/162329b0.
70. Hayashida M, Cui K, Homeniuk D, Phengchat R, Blackburn AM, Malac M. Parameters affecting the accuracy of nanoparticle shape and size measurement in 3D. Micron 2019;123:102680. https://doi.org/10.1016/J.MICRON.2019.102680.
71. Radnik J, Kersting R, Hagenhoff B, Bennet F, Ciornii D, Nymark P, et al. Reliable surface analysis data of nanomaterials in support of risk assessment based on minimum information requirements. Nanomaterials 2021;11:1–20. https://doi.org/10.3390/nano11030639.
72. Greczynski G, Hultman L. X-ray photoelectron spectroscopy: Towards reliable binding energy referencing. Prog Mater Sci 2020;107:100591. https://doi.org/10.1016/J.PMATSCI.2019.100591.
73. Lebugle A, Axelsson U, Nyholm R, Mprtensson N. Experimental L and M Core Level Binding Energies for the Metals 22Ti to 30Zn. Phys Scr 1981;23:825. https://doi.org/10.1088/0031-8949/23/5A/013.
74. Romero R, López-Ibáñez R, Dalchiele EA, Ramos-Barrado JR, Martín F, Leinen D. Compositional and physico-optical characterization of 0–5% Al-doped zinc oxide films prepared by chemical spray pyrolysis. J Phys D Appl Phys 2010;43:095303. https://doi.org/10.1088/0022-3727/43/9/095303.
75. Al-Gaashani R, Radiman S, Al-Gaashani R, Radiman S, Daud AR, Tabet N, et al. XPS and optical studies of different morphologies of ZnO nanostructures prepared by microwave methods. Elsevier 2012. https://doi.org/10.1016/j.ceramint.2012.08.075.
76. Crist BV. XPS in industry—Problems with binding energies in journals and binding energy databases. J Electron Spectros Relat Phenomena 2019;231:75–87. https://doi.org/10.1016/J.ELSPEC.2018.02.005.
77. Johansson B, Mårtensson N. Core-level binding-energy shifts for the metallic elements. Phys Rev B 1980;21:4427. https://doi.org/10.1103/PhysRevB.21.4427.
78. Sevier KD. Atomic electron binding energies. At Data Nucl Data Tables 1979;24:323–71. https://doi.org/10.1016/0092-640X(79)90012-3.
79. Shirley DA, Martin RL, Kowalczyk SP, McFeely FR, Ley L. Core-electron binding energies of the first thirty elements. Phys Rev B 1977;15:544. https://doi.org/10.1103/PhysRevB.15.544.
80. Fadley CS, Hagstrom SBM, Klein MP, Shirley DA. Chemical Effects on Core-Electron Binding Energies in Iodine and Europium. J Chem Phys 1968;48:3779–94. https://doi.org/10.1063/1.1669685.
81. Bagga S, Akhtar J, Mishra S. Synthesis and applications of ZnO nanowire: A review. AIP Conf Proc, vol. 1989, American Institute of Physics Inc.; 2018. https://doi.org/10.1063/1.5047680.
82. Yassin MT, Mostafa AAF, Al-Askar AA, Al-Otibi FO. Facile Green Synthesis of Zinc Oxide Nanoparticles with Potential Synergistic Activity with Common Antifungal Agents against Multidrug-Resistant Candidal Strains. Crystals (Basel) 2022;12. https://doi.org/10.3390/cryst12060774.
83. Minhas LA, Mumtaz AS, Kaleem M, Farraj D Al, Kamal K, Minhas MAH, et al. Green Synthesis of Zinc Oxide Nanoparticles Using Nostoc sp. and Their Multiple Biomedical Properties. Catalysts 2023;13. https://doi.org/10.3390/catal13030549.

84. Albiss B, Abu-Dalo M. Photocatalytic degradation of methylene blue using zinc oxide nanorods grown on activated carbon fibers. Sustainability (Switzerland) 2021;13. https://doi.org/10.3390/su13094729.
85. Modi S, Fulekar MH. Synthesis and characterization of zinc oxide nanoparticles and zinc oxide/cellulose nanocrystals nanocomposite for photocatalytic degradation of Methylene blue dye under solar light irradiation. Nanotechnology for Environmental Engineering 2020;5:18. https://doi.org/10.1007/s41204-020-00080-2.
86. Momeni A, Meshkatalsadat MH, Bakhtiari Shahin B, Mousavi Y. Photodegradation of methylene blue by phytosynthesized Ag–ZnO nanocomposites. Hybrid Advances 2023;3:100050. https://doi.org/10.1016/J.HYBADV.2023.100050.
87. Waseem S, Sittar T, Kayani ZN, Gillani SSA, Rafique M, Asif Nawaz M, et al. Plant mediated green synthesis of zinc oxide nanoparticles using Citrus jambhiri lushi leaves extract for photodegradation of methylene blue dye. Physica B Condens Matter 2023;663:415005. https://doi.org/https://doi.org/10.1016/j.physb.2023.415005.
88. Sedefoglu N. Characterization and photocatalytic activity of ZnO nanoparticles by green synthesis method. Optik (Stuttg) 2023;288:171217. https://doi.org/https://doi.org/10.1016/j.ijleo.2023.171217.
89. Haspulat Taymaz B, Demir M, Kamış H, Orhan H, Aydoğan Z, Akıllı A. Facile and green synthesis of ZnO nanoparticles for effective photocatalytic degradation of organic dyes and real textile wastewater. Int J Phytoremediation 2023;25:1306–17. https://doi.org/10.1080/15226514.2022.2150142.
90. Nawaz R, Ullah H, Ghanim AAJ, Irfan M, Anjum M, Rahman S, et al. Green Synthesis of ZnO and Black TiO2 Materials and Their Application in Photodegradation of Organic Pollutants. ACS Omega 2023;8:36076–87. https://doi.org/10.1021/acsomega.3c04229.
91. Ramasubramanian A, Selvaraj V, Chinnathambi P, Hussain S, Ali D, Kumar G, et al. Enhanced photocatalytic degradation of methylene blue from aqueous solution using green synthesized ZnO nanoparticles. Biomass Convers Biorefin 2023;13:17271–82. https://doi.org/10.1007/s13399-023-04992-2.
92. Khan I, Saeed K, Zekker I, Zhang B, Hendi AH, Ahmad A, et al. Review on Methylene Blue: Its Properties, Uses, Toxicity and Photodegradation. Water (Switzerland) 2022;14. https://doi.org/10.3390/w14020242.
93. U.S Code of Federal Regulations. Food and Drugs-Zinc Oxide. vol. 3. Silver Spring-10903 New Hampshire Avenue: Code of Federal regulations; 2022.
94. Zakari A, Khan I, Tan D, Alvarado R, Dagar V. Energy efficiency and sustainable development goals (SDGs). Energy 2022;239:122365. https://doi.org/10.1016/J.ENERGY.2021.122365.
95. Fuso Nerini F, Sovacool B, Hughes N, Cozzi L, Cosgrave E, Howells M, et al. Connecting climate action with other Sustainable Development Goals. Nature Sustainability 2019 2:8 2019;2:674–80. https://doi.org/10.1038/s41893-019-0334-y.
96. Pearce JM. Teaching Science by Encouraging Innovation in Appropriate Technologies for Sustainable Development Peer-Reviewed Papers Ethical Requirement for Service Learning for Sustainable Development. Hal-02120521 2017:1–10.